

Ada3Diff: Defending against 3D Adversarial Point Clouds via Adaptive Diffusion

Kui Zhang¹ Hang Zhou² Jie Zhang^{1,3} Qidong Huang¹
 Weiming Zhang¹ Nenghai Yu¹

University of Science and Technology of China¹ Simon Fraser University² University of Waterloo³

Abstract

Deep 3D point cloud models are sensitive to adversarial attacks, which poses threats to safety-critical applications such as autonomous driving. Robust training and defend-by-denoise are typical strategies for defending adversarial perturbations, including adversarial training and statistical filtering, respectively. However, they either induce massive computational overhead or rely heavily upon specified noise priors, limiting generalized robustness against attacks of all kinds. This paper introduces a new defense mechanism based on denoising diffusion models that can adaptively remove diverse noises with a tailored intensity estimator. Specifically, we first estimate adversarial distortions by calculating the distance of the points to their neighborhood best-fit plane. Depending on the distortion degree, we choose specific diffusion time steps for the input point cloud and perform the forward diffusion to disrupt potential adversarial shifts. Then we conduct the reverse denoising process to restore the disrupted point cloud back to a clean distribution. This approach enables effective defense against adaptive attacks with varying noise budgets, achieving accentuated robustness of existing 3D deep recognition models.

1. Introduction

With the easy affordability of 3D sensors, 3D data has been widely used in different areas such as autonomous driving, virtual reality, and robotics, to help perception systems for better scene understanding. Among diverse 3D data forms, 3D point-cloud representation plays a significant role, which depicts the geometric information of the 3D object and does not consume much computational memory even with high resolution. Recently, an increasing amount of studies have demonstrated tremendous success in using deep models for large-scale 3D point cloud analysis, such as classification and semantic segmentation. However, it has been demonstrated that deep models can be easily misled by adversarial point clouds. For example, with a carefully designed optimization strategy [7, 8, 12, 25, 29, 33], the at-

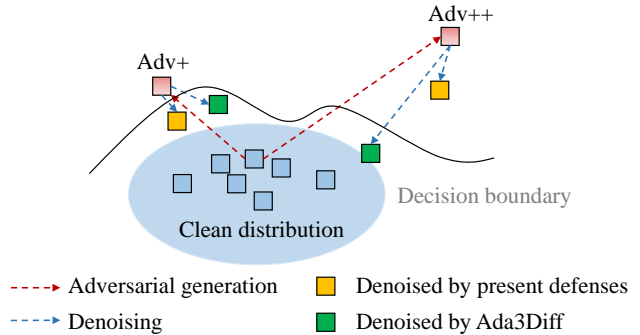


Figure 1. Comparison of our Ada3Diff with present defenses on the high-level feature space. For varying distorted adversarial point clouds, Ada3Diff obtains denoised point clouds closer to the clean distribution than others. Adv+ and Adv++ denote the adversarial attacks with slight and large distortions, respectively.

tacker can directly shift points on the 3D surfaces to generate adversarial point clouds, which can preserve the original 3D shapes to bypass human inspection and can even transfer attack ability across different models. These attacks pose a significant threat to safety-critical applications.

To alleviate this issue, two main defense strategies have been proposed. One is dedicated to training a robust classifier to capture discriminative features for analysis [3, 11, 23]. Commonly, we obtain the robust classifier by fine-tuning the original classifier or training it from scratch, both of which will introduce massive computational costs. The other one is to append a denoising module before the well-trained model to eliminate the effect of adversarial noises [31, 39]. Despite of easy plug-in-and-play and model-agnostic properties, it is inapplicable for denoising adversarial point clouds under different noise budgets as it depends heavily on the specified noise prior. Moreover, defense methods based on such strategy will induce an unsatisfying performance degradation facing larger adversarial noises. In Figure 1, we visualize the high-level feature space of present defenses vs. ours. The performance of existing defenses are limited by 1) it cannot effectively push the denoised point cloud back to the clean distribution; 2) it

cannot handle the adversarial point cloud with a large distortion. Taking the state-of-the-art defense IF-Defense [31] as an example, we find that it achieves a satisfying performance on point clouds with slight distortions. However, it fails on large distortion cases, which inherently violate its basic assumption of preserving surface continuity for robust recognition.

In this paper, we present a novel defense framework, Ada3Diff, to reconstruct adversarial point clouds by diffusion probabilistic models, which can intrinsically move diverse adversarial distributions back to the corresponding clean distribution. Specifically, we first perform forward diffusion on the target input to randomly perturb the potential adversarial noise. Then, the perturbed input will be transformed into a clean distribution by reverse denoising. During the diffusion process, a large time step is not conducive to the reconstruction of shape-invariant adversarial point clouds, while a small time step is not effective in eliminating the adversarial noise. Therefore, the main challenge is to determine a suitable diffusion time step in advance.

To overcome this challenge, we design a distortion estimation strategy to evaluate all types of inputs including clean and adversarial point clouds. Specifically, we calculate the distance of each point from its neighborhood fitting plane and determine the diffusion time step based on the average distance over the entire point set, which is inspired by the observation that non-shape-invariant point clouds tend to be more locally chaotic.

Extensive experiments demonstrate that our Ada3Diff outperforms existing defense methods in terms of robustness against attacks of all kinds, especially facing with large adversarial noise. Besides, we provide a comprehensive evaluation to showcase the effectiveness of our method on different datasets, models, and even attack scenarios. Finally, some ablation studies are conducted to verify our design.

In summary, our contributions are three-fold:

- We propose a novel defense approach against adversarial 3D point cloud, based on the diffusion model that has excellent modeling capability of the data distribution, which can effectively defend against adversarial attacks with various distortions.
- We design a distortion estimation strategy to approximate the local distortion strength, which can adaptively choose different diffusion time steps to further improve the robust classification performance.
- Extensive experiments show that our method outperforms current defense methods by a large margin facing with large distortions, and meanwhile it achieves comparable performance on point clouds with slight distortions.

2. Related Works

2.1. 3D Point Cloud Recognition

According to network structures, the existing deep-learning-based models for 3D point cloud recognition can be roughly classified into MLP-based, graph-based, convolution-based, and transformer-based methods. In the following part, we introduce one classic example for each category, respectively. PointNet [19] pioneered the extraction of features for each point individually, and then fused features with a symmetric function for subsequent classification. However, it mainly focuses on the fusion of global features and cannot effectively capture the local structure of spatial points. By contrast, DGCNN [28] dynamically selects neighbors for each point based on the feature embedding in each layer and applies edge convolution to extract local structural features. Concurrently, PointConv [30] designed a convolution operation for the irregular grid that can efficiently extract local features from 3D point clouds. Inspired by the success of transformers in the field of computer vision and NLP, PCT [6] introduces self-attention into point clouds recognition, which can handle unstructured unordered data and extract contextual features very well. Very recently, CurveNet [34] achieved excellent classification performance, which designed a novel curve grouping and aggregation module that can effectively capture the shape and geometric features of point clouds. In this paper, we adopt CurveNet as the default target model for robustness comparison, and the other models mentioned above are used to verify the scalability of our method.

2.2. 3D Point Cloud Attacks

In addition to guaranteeing the attack performance, existing 3D point cloud attack methods [7–9, 12, 21, 25, 29, 33, 38] target satisfying other two requirements, *i.e.*, imperceptibility and transferability. For imperceptibility, the famous gradient-based method PGD [16] can be adjusted for a slight distortion, while 3D-Adv [33] can append additional distance constraints to limit perceptible perturbations. To support the adversarial point clouds for better surface reconstruction, k NN-Adv [25] introduced an extra k NN loss for its optimization objective. Differently, Point dropping [37] deleted the most important points based on the saliency map. All above methods can generate adversarial point clouds that have smooth surfaces and smaller average perturbation distances. To improve transferability, attack methods such as AdvPC [7] and AOF [12] generated adversarial point clouds that tend to have a large degree of local disorganization, manifested by a more uniform distribution of local points within the sphere. Both attack methods sacrificed imperceptibility for transferability. In this paper, we utilize all these methods mentioned above to evaluate robustness against attacks with various distortions.

2.3. 3D Point Cloud Defenses

3D Point Cloud Defenses are mainly achieved by building robust classifiers or purifying adversarial point clouds. [3, 11, 13, 23] construct classification models that are robust against adversarial point clouds by designing robust training methods or designing robust recognition modules and networks. However, all these methods will induce high computational cost and are model-specific. Another route is to denoise the adversarial point clouds before feeding it to the model, which is model-agnostic and can be combined with various robust training methods. Simple random sampling (SRS) [35] is a commonly-used solution to purify adversarial point clouds. Another common method, called statistical outlier removal (SOR) [20], assumed the adversarial points as the outliers. Based on the SOR, DUP-Net [39] further supplemented the information with an additional up-sampling network. However, these methods cannot handle adversarial points that deviate too far from the clean distribution. Afterward, IF-Defense [31] utilized implicit functions and distribution-aware loss to constrain the SOR-processed points to be distributed as evenly as possible over the surface, achieving good performance against a variety of attacks, yet it performs poorly suffering larger distortions, due to that the constrains of an even surface cannot guarantee that the point clouds purified back to the natural distribution.

2.4. Diffusion Probabilistic Models

Inspired by nonequilibrium thermodynamics, the diffusion probabilistic model [22] is proposed to model the process of generating data as a gradual denoising process based on Markov chains. Recent work [15, 40] has demonstrated the success of using diffusion models to model the generation of point clouds, which pointed out that the reverse diffusion process can gradually eliminate noise of different variances to generate point clouds similar to the clean data distributions. In addition, some recent work [17, 27] used diffusion models to remove adversarial noise on images and achieves performance comparable to adversarial training. In this paper, we pioneer exploring the powerful diffusion probabilistic models to defend against 3D point clouds attacks, and further introduce the distortion estimation for adaptive defense.

3. Method

In this section, we first provide the formulation of diffusion models and clarify the threat model. Then, we introduce the proposed Ada3Diff in detail.

3.1. Preliminary

Formulation of diffusion models. Given a point cloud $\mathbf{x} \in \mathbb{R}^{N \times 3}$ sampled from a real-data distribution $q(\mathbf{x})$, the

diffusion process consists of a Markov process can be parameterized as Gaussian form:

$$q(\mathbf{x}_t | \mathbf{x}_{t-1}) = \mathcal{N}(\mathbf{x}_t; \sqrt{1 - \beta_t} \mathbf{x}_{t-1}, \beta_t \mathbf{I}), \quad (1)$$

where $\beta_t \in [0, 1]$ for $t \in [1, T]$ is a constant that controls the noise step size. From the good properties of Markov and Gaussian distributions, the diffusion expression of \mathbf{x}_t at the t step can be easily obtained from \mathbf{x}_0 :

$$\mathbf{x}_t = \sqrt{\bar{\alpha}_t} \mathbf{x}_0 + \sqrt{1 - \bar{\alpha}_t} \epsilon, \epsilon \sim \mathcal{N}(0, \mathbf{I}), \quad (2)$$

where $\alpha_t = 1 - \beta_t$ and $\bar{\alpha}_t = \prod_{i=1}^t \alpha_i$. The reverse process then learns the stepwise denoising through a neural network p_θ , again defined as a Markov process with Gaussian transitions:

$$\begin{aligned} p_\theta(\mathbf{x}_{0:T}) &= p(\mathbf{x}_T) \prod_{t=1}^T p_\theta(\mathbf{x}_{t-1} | \mathbf{x}_t), \\ p_\theta(\mathbf{x}_{t-1} | \mathbf{x}_t) &= \mathcal{N}(\mathbf{x}_{t-1}; \mu_\theta(\mathbf{x}_t, t), \sigma_t^2 \mathbf{I}), \end{aligned} \quad (3)$$

where the variance σ_t^2 can be left out of the training. After training, randomly sampled Gaussian data points can be gradually generated into a real point cloud by p_θ .

Threat model. For an input point cloud $\mathbf{x} \in \mathbb{R}^{N \times 3}$ containing N points, the attacker \mathcal{A} aims to mislead the classifier f by modifying \mathbf{x} under a certain perturbation budget \mathbb{B}_ξ :

$$f(\mathcal{A}(\mathbf{x})) \neq f(\mathbf{x}), \text{ s.t. } |\mathcal{A}(\mathbf{x}) - \mathbf{x}| \subseteq \mathbb{B}_\xi, \quad (4)$$

where ξ is the distance measurement for adversarial shifts, or the number of the dropped points for point dropping.

Furthermore, we clarify 1) the ability of attackers and 2) our defense goal as follows: 1) For defense methods integrated before the classifier input, when the attacker has access to all the information of the classifier without the knowledge of the preprocessor, it can be considered as a gray-box attack. When the attacker has all the knowledge of the preprocessor and the classifier, then a white-box attack can be performed. 2) As shown in Figure 2, given an adversarial point cloud $\mathbf{x}^{adv} = \mathcal{A}(\mathbf{x})$, Ada3Diff aims to purify it back to the clean distribution for correct prediction.

3.2. The Proposed Ada3Diff

Motivation. At the macro level, the well-trained diffusion model can generate point clouds belonging to the real data distribution, and at the micro level, each step of diffusion and denoising will introduce the random Gaussian noise, which may disrupt adversarial perturbations and recover the input to the correct distribution. Both characteristics satisfy our defense goal mentioned above.

According to the former discussion, we observe that different attacks generate adversarial point clouds with different levels of distortion. For imperceptible adversarial point

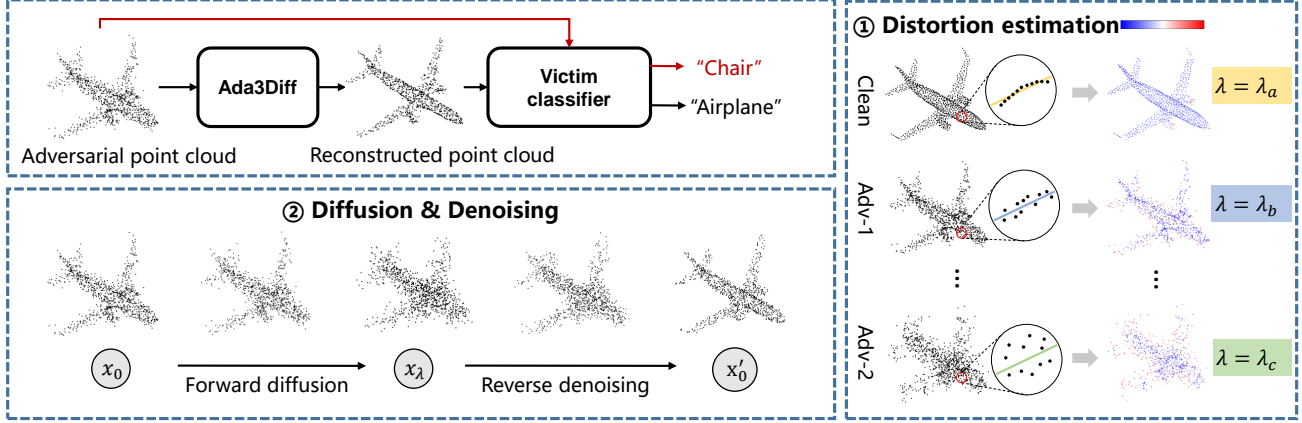


Figure 2. The overall framework of the proposed Ada3Diff, which consists of ① distortion estimation and ② diffusion & denoising. For an input point clouds x_0 , we first estimate the distortion according to the distance of each point from its neighborhood best-fit plane where color closer to red represents a higher degree of confusion. We adaptively choose different diffusion time steps λ ($\lambda_a < \lambda_b < \lambda_c$) for forward diffusion and then recover the clean distribution of the x_0 by reverse denoising.

clouds, a relatively less time steps should be used to mainly adjust the point distribution and preserve more local structure details, while for adversarial point clouds with larger distortions, more time steps can destroy the larger noise and restore them back to the clean data distribution. To perform adaptive diffusion-based denoising of adversarial point clouds, we employ a perturbation measurement approach to perform distortion estimation on the adversarial point cloud before diffusion process.

Distortion estimation. Imperceptible perturbations tend to move along the surface, while perturbations with large distortions are the opposite and have a larger average distance from the origin set. This chaos is specifically manifested by a more uniform distribution of local point sets within the sphere. Inspired by [5], we approximate the confusion degree by fitting the best plane of the local neighborhood and calculating the distance of the point set to this plane.

Mathematically, a subset $\mathbf{x}_{sub} \in \mathbb{R}^{K \times 3}$ containing K points from \mathbf{x} are first selected, where $x_i \in \mathbb{R}^3$ is the center point and the other points $x_j \in \mathcal{N}(x_i)$ are the non-repeating $K - 1$ nearest neighbors of x_i . Our goal is to find an optimal plane for fitting the neighborhood points such that the sum of the distances from the points in \mathbf{x}_{sub} to this plane is minimized. Formally, a plane \mathbf{p} is determined by its normal vector $\mathbf{n} = (n_x, n_y, n_z)^T$ and a point $p' = (p_x, p_y, p_z)$ on the plane:

$$\mathbf{p} : \mathbf{n}^T \cdot (p - p') = 0. \quad (5)$$

The normal vector of the fitted plane can be obtained by

minimizing the objective L_d as follows:

$$\begin{aligned} L_d &= \sum_{x_j \in \mathbf{x}_{sub}} \|\mathbf{n}^T \cdot (x_j - p')\| \\ &= \|\mathbf{x}'_{sub} \cdot \mathbf{n}\|, s.t. \|\mathbf{n}\|_2 = 1, \end{aligned} \quad (6)$$

where \mathbf{x}'_{sub} is the matrix that consists of each point of \mathbf{x}_{sub} minus the coordinate p' . By calculating the partial derivative of p' , we can conclude that $p' = \frac{1}{|\mathbf{x}_{sub}|} \sum_{x \in \mathbf{x}_{sub}} x_j$ is the center of mass of the point in the neighborhood. By performing the singular decomposition of \mathbf{x}'_{sub} , i.e., $\mathbf{x}'_{sub} = U\Sigma V^H$, we can easily observe that the vector corresponding to the last column of V is the normal vector corresponding to the fitted plane. Based on this, we can calculate the distance from the current point x_i to the plane by $\mathbf{n}^T \cdot (x_i - p')$ or the sum of the distances from all points in the \mathbf{x}_{sub} to the plane as an estimate of the distortion of the point x_i . Finally, we take the mean of distortion estimates of all points denoted as \mathcal{E}_x , as an approximation to the degree of perturbation of the whole point cloud \mathbf{x} .

Diffusion and denoising. Our diffusion-based denoising can be divided into two steps, which correspond to the forward diffusion process and the reverse denoising process. Specifically, given a point cloud $\mathbf{x}_0^{adv} \in \mathbb{R}^{N \times 3}$ with noise that can mislead the classification, we first perform forward diffusion on it by λ time steps according to equation 2:

$$\begin{aligned} \mathbf{x}_\lambda^{adv} &= \sqrt{\alpha_\lambda} \mathbf{x}_0^{adv} + \sqrt{1 - \alpha_\lambda} \epsilon \\ &= \sqrt{\alpha_\lambda} \mathbf{x}_0 + \sqrt{\alpha_\lambda} \delta + \sqrt{1 - \alpha_\lambda} \epsilon, \end{aligned} \quad (7)$$

where δ satisfies a certain perturbation budget \mathbb{B}_{eps} . Each point in the point cloud is weighted with a superposition of

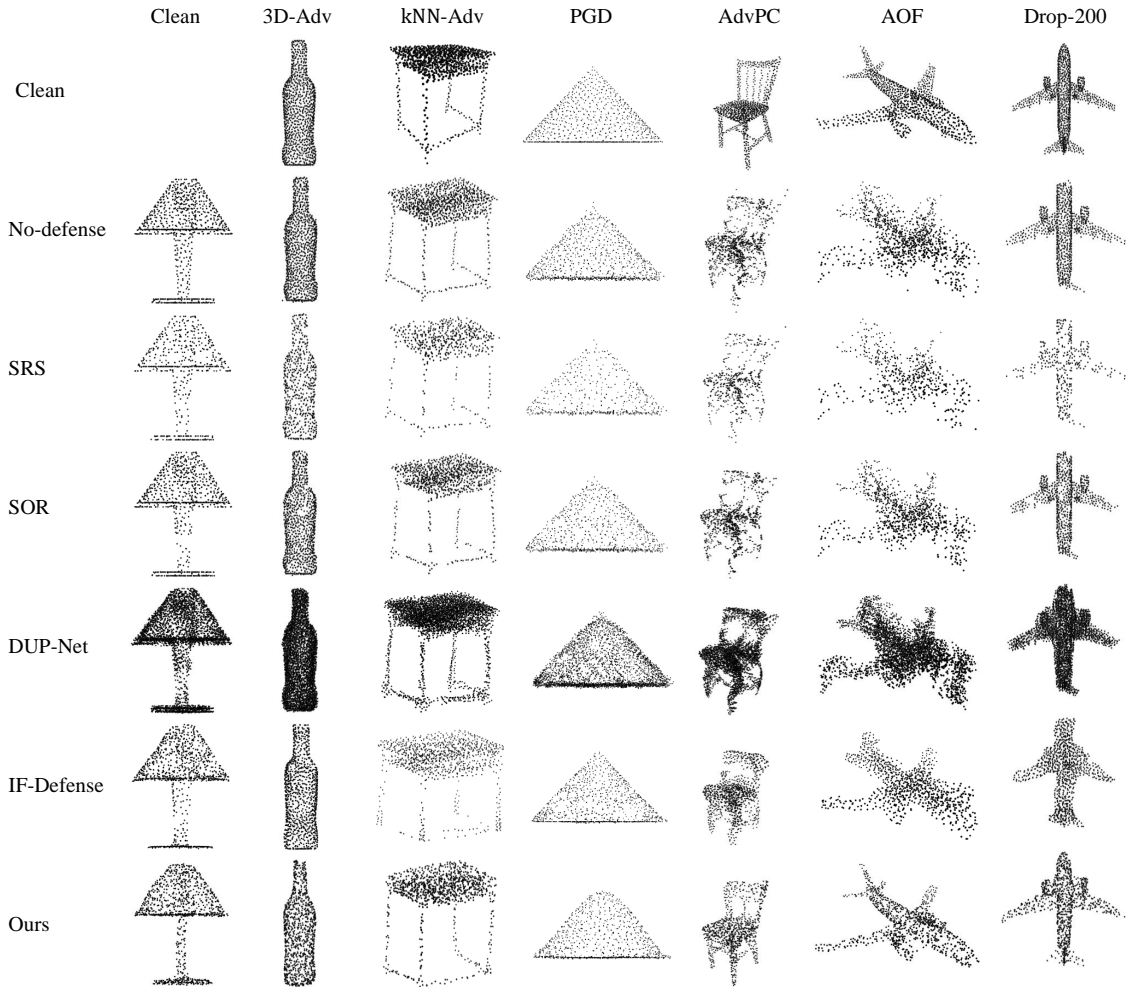


Figure 3. Qualitative comparison of reconstruction results of different defense methods against diverse adversarial point clouds. The first row of each column is the clean point cloud corresponding to the reconstruction result. The first column is the result of the reconstruction of the clean point cloud.

independent random Gaussian noise, which counteracts the effect of the perturbation to some extent, as demonstrated in [35]. Furthermore, the forward diffusion is also used to make the starting point of the reverse process as consistent as possible with the input distribution of the Markov kernel at step λ . After that, we take \mathbf{x}_λ^{adv} as the starting point and progressively eliminate the noise by $p_\theta(\mathbf{x}_{t-1}|\mathbf{x}_t)$. Finally, we output a point cloud \mathbf{x}'_0 that is close to the clean data distribution, and then feed it to the classifier.

In the process of diffusion and denoising, it is important to choose an appropriate maximum time step λ for forward diffusion. As λ increases, the point cloud gradually becomes noisy and the local structural details become increasingly coarse due to the decreasing weight $\sqrt{\alpha_\lambda}$ and the gradually increasing proportion of Gaussian noise. Therefore, a relatively small time step should be chosen to pre-

serve the coarse local structure details and eliminate the adversarial perturbation as much as possible. After we determine the confidence interval of the Gaussian distribution ϵ in Equation 7, we choose the λ that can exactly make the weighted Gaussian noise larger than the weighted predetermined budget as the maximum diffusion time step.

In order to obtain the adaptive time step λ by distortion estimation, we first calculate \mathcal{E}_x of all clean point clouds in the dataset and get the distortion distribution \mathcal{D} of the whole clean dataset. Then, we quarter the distribution \mathcal{D} as $\mathcal{D}_1, \mathcal{D}_2, \mathcal{D}_3$, and \mathcal{D}_4 in turn. Similarly, we quarter the maximum diffusion time step λ as $\lambda_1, \lambda_2, \lambda_3$, and λ_4 , respectively. Finally, given a target point cloud \mathbf{x}_i , we select the corresponding time step λ_i based on the distortion range \mathcal{D}_i , which the $\mathcal{E}_{\mathbf{x}_i}$ belongs to. The above strategy is reasonable, because the clean point cloud with a large local curvature or

| Attacks | Clean | 3D-Adv | kNN-Adv | PGD | AdvPC | AOF | Drop-200 |
|-------------------------|-------------|-------------|-------------|-------------|-------------|-------------|-------------|
| CD ($\times 10^{-4}$) | 0 | 0.59 | 1.20 | 6.35 | 17.2 | 21.3 | 11.0 |
| No defense | 92.3 | 0 | 7.21 | 0 | 0.85 | 0 | 75.2 |
| SRS [35] | 86.8 | 84.9 | 82.6 | 74.8 | 26.8 | 18.2 | 57.7 |
| SOR [20] | 91.0 | 88.1 | 78.2 | 64.0 | 16.9 | 8.27 | 78.8 |
| DUP-Net [39] | 88.8 | 88.0 | 85.3 | 79.5 | 49.4 | 31.6 | 74.2 |
| IF-Defense [31] | 86.7 | 86.6 | 85.7 | 83.7 | 62.3 | 47.3 | 77.6 |
| Ada3Diff | 88.4 | 87.7 | 87.2 | 87.6 | 85.9 | 85.4 | 78.1 |

Table 1. Comparison of robust classification accuracy on ModelNet40 under different attacks.

the presence of multiple surfaces in relatively close proximity can also make the \mathcal{E}_{x_i} large. By adaptive diffusion and denoising, we expect to preserve more local structures for point clouds with good surface properties and improve their classification accuracy.

4. Experiment

4.1. Experimental Setup

Datasets and recognition models. We adopt ModelNet40 [32] as the default dataset for comparison and main experiments. Besides, we also leverage ShapeNet Part [36] dataset to verify the generality of Ada3Diff. More details can be found in the appendix.

For point cloud recognition models, we utilize CurveNet [34] for comparison and demonstrate generality by other classic architectures including PointNet [19] based on MLP, DGCNN [28] based on graph convolution, PCT [6] using transformer, and PointConv [30] based on convolution.

Adversarial attacks and the baseline defenses. We selected attack methods with different imperceptibility, namely 3D-Adv [33], k NN-Adv [25], PGD [3, 16], AdvPC [7], AOF [12] and point dropping [37]. We constrain the maximum perturbation distance of all attacks except point dropping to be set to $l_\infty = 0.18$. More specific attack parameters are provided in the appendix.

We compare the proposed method with the baseline defense methods that also target pre-processing the adversarial point cloud before recognition, including SRS [35], SOR [20], DUP-Net [39] and IF-Defense [31], where SOR we refer to the implementation in DUP-Net [39]. We follow the default settings in their original paper or released code. More details can be found in the appendix.

Implementation details. Following the PVD [40], we use point-voxel CNN [14] as the backbone network of the

| | 3D-Adv | kNN-Adv | PGD | AdvPC | AOF |
|------------|--------|---------|------|-------|-------|
| IF-Defense | 5.48 | 8.66 | 4.47 | 8.33 | 19.38 |
| Ours | 5.26 | 5.87 | 4.56 | 3.48 | 4.94 |

Table 2. JSD between the purified and clean point clouds, the smaller the value means the closer the distribution between them. JSD here is multiplied by 10^4 .

| Attack | SRS | SOR | DUP-Net | IF-Defense | Ada3Diff |
|----------|------|------|---------|------------|-------------|
| BPDA-PGD | 12.6 | 15.5 | 22.6 | 32.0 | 72.8 |

Table 3. Robust classification accuracy against the BPDA-based white-box attack on ModelNet40.

diffusion model and train the diffusion models on ModelNet40 and ShapeNet Part, respectively. We select the 10 nearest neighbors around each point to estimate the distortion. We determine 99.8% as the confidence interval of the Gaussian distribution in Equation 7, namely, set $\lambda = 20$ as the maximum diffusion time steps. We empirically operate 4 rounds of Ada3Diff iteratively to further eliminate perturbations and improve the safety of denoising with less time steps.

Evaluation metrics. In this paper, we mainly focus on the robustness evaluation. For this, we adopt robust classification accuracy, which is defined as the classification accuracy of the set of samples that purified by defense methods. We use the Jensen-Shannon Divergence (JSD) [1] to measure the distribution distance between the reconstructed point cloud and the original point cloud set. We use the average Chamfer distance (CD) [4] between the adversarial point cloud and the original point cloud to measure the perturbation intensity. Higher CD means larger distortions.

| Defenses | Clean | 3D-Adv | kNN-Adv | PGD | AdvPC | AOF | Drop-200 |
|------------|-------|--------|---------|------|-------|------|----------|
| No defense | 98.5 | 0 | 16.6 | 8.94 | 15.0 | 0.14 | 87.9 |
| Ada3Diff | 98.2 | 97.9 | 98.0 | 98.0 | 97.4 | 96.8 | 91.7 |

Table 4. Robustness evaluation on ShapeNet Part under different attacks.

| Models | No defense | Clean | 3D-Adv | kNN-Adv | PGD | AdvPC | AOF | Drop-200 |
|----------------|------------|-------|--------|---------|------|-------|------|----------|
| PointNet [19] | 89 | 86.9 | 86.9 | 86.2 | 85.9 | 85.0 | 84.1 | 55.1 |
| DGCNN [28] | 92.3 | 87.2 | 86.7 | 86.4 | 85.9 | 85.9 | 85.3 | 75.6 |
| PCT [6] | 92.7 | 87.6 | 87.6 | 86.9 | 86.5 | 85.5 | 85.8 | 71.8 |
| PointConv [30] | 91.9 | 86.8 | 85.5 | 85.6 | 86.3 | 83.4 | 83.5 | 68.9 |
| CurveNet [34] | 92.3 | 88.4 | 87.7 | 87.2 | 87.6 | 85.9 | 85.4 | 77.8 |

Table 5. Robustness evaluation against various attacks on different models. All experiments are conducted on ModelNet40.

4.2. Comparison with the Baseline Defense Methods

Robustness against various attacks. In Table 1, we provide the comparison of the robust classification accuracy with the baseline defense methods under different adversarial attacks. It can be seen that the proposed Ada3Diff performs well in most cases and outperforms other defense methods by a large margin especially suffering adversarial attacks with severe distortion, such as AdvPC and AOF. The proposed method can achieve a comparable performance to the best defense for attacks with slight distortions, such as 3D-Adv, kNN-Adv, and PGD. For the special attack Drop-200 that removing 200 important points based on the saliency map, all defense methods perform poorly, where our performance is still acceptable.

In Figure 3, we provide some visual examples of the purified point clouds by different defenses under different attacks. Consistent with the quantitative results shown in Table 1, Ada3Diff achieves an excellent reconstruction suffering attacks with large distortions, while guaranteeing a comparable performance facing with imperceptible adversarial attacks. Moreover, Table 2 shows the JSD comparison between our method and IF-Defense, which again verifies that the proposed method reconstructs large distorted point clouds closer to the distribution of clean point clouds.

4.3. Comprehensive Evaluation on Ada3Diff

Evaluation on different datasets. Table 4 shows the robust classification accuracy of Ada3Diff on the ShapeNet Part dataset. The proposed approach still shows superb defense performance against different attacks.

Evaluation on different models. To further evaluate the generality of the proposed approach to different models, we conducted experiments on point cloud recognition networks

with different architectures. As shown in Table 5, the robust classification accuracy under different attacks other than point dropping is basically above 85% for all recognition models. Because these recognition models focus on different spatial relationships, containing global relationships as well as local correlations from various local aggregation operations, it means that the recovered point cloud is well reconstructed in terms of both local structural feature and global consistency.

Evaluation on different attack scenarios. We use a simple Backward Pass Differentiable Approximation (BPDA) [2] based PGD attack to evaluate the performance of the proposed method under the white-box scenario. Assuming that the point cloud permutation after Ada3Diff purified is unchanged, we use BPDA to obtain the approximate gradient of the purified point cloud with respect to the input, so as to perform PGD attack in an end-to-end manner. We increase the number of gradient descents to 100. In Table 3, we find that Ada3Diff can still preserve the robust accuracy at 72.8%, while other defenses suffer a great degradation.

The influence of diffusion time steps and Ada3Diff rounds. In Figure 4(a) and 4(b), we demonstrate our assumption that the optimal diffusion time steps are different for attacks with different distortions. As mentioned above, Ada3Diff achieves better performance fed with large distortions compared with small distortions. We explain that it is because that the selection strategy for time steps is not precise enough especially for slight distortions, which suggests that there still exists a potential performance improvement of Ada3Diff by better designs and strategies. In our experiments, we set Ada3Diff rounds as 4 by default, we further consider different rounds to evaluate its influence.

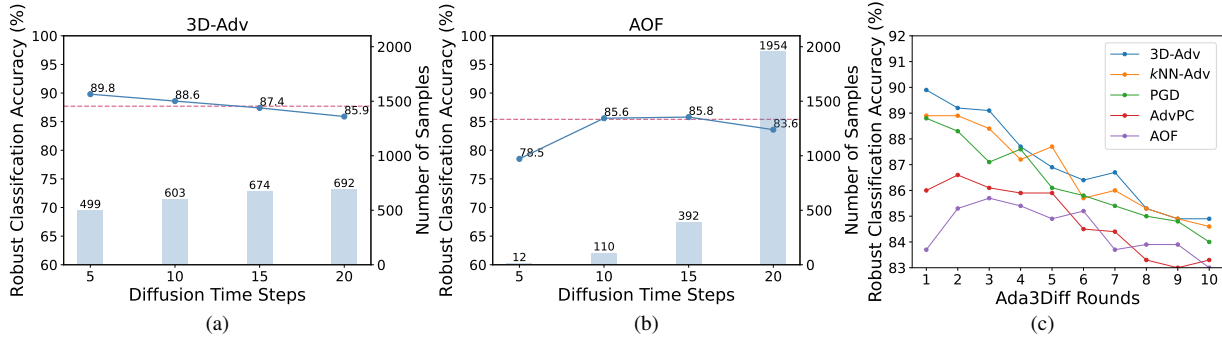


Figure 4. The influence of the diffusion time steps and Ada3Diff rounds. In (a) and (b): blue line means the robustness against attacks with a fixed diffusion time steps, where red dashed line represents the corresponding performance of Ada3Diff. We also show the sampling numbers of each time step by Ada3Diff. (c) shows the performance of the defense with different Ada3Diff rounds against different attacks.

Figure 4(c) shows that more Ada3Diff rounds will induce a degradation of clean accuracy, while less rounds cannot resist against attacks with large distortions such as AOF. We find Ada3Diff rounds from 2 to 4 has better defense performance, which can be flexibly selected in practice.

Visualization of latent distribution. We select 15 classes, each with 100 randomly selected samples, and visualize the distribution over the latent space using t-SNE [26]. Figure 5 and Figure 7 in the appendix show the distribution of low-dimensional manifolds for different types of samples in the feature space of the model. The point clouds reconstructed by other methods are aliased between different classes in the hidden space of the model, while the features extracted from the point clouds reconstructed by our method are still separable in the latent space and the distribution is more similar to that of clean point clouds, indicating that the local structure of the point clouds is better reconstructed.

5. Discussion

Difference with PointDP [24]. A concurrent work called PointDP [24] also utilizes a diffusion probabilistic model for defense of 3D adversarial point clouds. Broadly, PointDP employs a *conditional* diffusion probabilistic model that uses the encoded features of the adversarial point cloud as the conditional guidance and empirically chooses a *fixed* diffusion time step to incrementally denoise the adversarial point cloud. By comparison, Ada3Diff uses an unconditional diffusion probabilistic model as the pre-processing module and conducts distortion-adaptive diffusion and multi-round denoising. This is the fundamental differences between Ada3Diff and PointDP. For these differences, we argue that a common encoder may introduce additional adversarial risk since the conditions can significantly influence the direction of the diffusion model. Moreover, Ada3Diff can effectively defend against adver-

sarial point clouds with diverse distortion intensity. We claim that the adaptive strategy is a necessary component of the defense pipeline and hope it can shed some light on the defense methods based on the diffusion probabilistic model. More in depth, PointDP proposes a denoising pipeline drawing on the success of DiffPure[1] on image defense whereas we build a defense pipeline based on the diffusion model from a distribution perspective.

6. Conclusion

In this paper, we propose a novel 3D point cloud defense, named Ada3Diff, to reconstruct adversarial point clouds by adaptive diffusion and reverse denoising. The proposed Ada3Diff can be plugged into various classification networks to help robust recognition. Extensive experiments have demonstrated that Ada3Diff can effectively defend against point cloud attacks with various distortions. Specifically, we outperforms the current defense by a large margin suffering large distortions, meanwhile preserving a comparable performance facing with slight distortions. We shall point out that the proposed distortion estimation and diffusion step interval division belongs to a relatively coarse strategy, which will be studied to further improve the defense performance. Besides, how to enhance the robustness against the point dropping attack is also a research direction for our future work.

References

- [1] Panos Achlioptas, O. Diamanti, Ioannis Mitliagkas, and L. Guibas. Learning representations and generative models for 3d point clouds. In *ICML*, 2018. 6
- [2] Anish Athalye, Nicholas Carlini, and David A. Wagner. Obfuscated gradients give a false sense of security: Circumventing defenses to adversarial examples. In *Proceedings of the 35th International Conference on Machine Learning*, pages 274–283, 2018. 7, 11
- [3] Xiaoyi Dong, Dongdong Chen, Hang Zhou, Gang Hua, Weiming Zhang, and Nenghai Yu. Self-robust 3d point

- recognition via gather-vector guidance. In *2020 IEEE/CVF Conference on Computer Vision and Pattern Recognition (CVPR)*, pages 11513–11521. IEEE, 2020. 1, 3, 6
- [4] Haoqiang Fan, Hao Su, and Leonidas J Guibas. A point set generation network for 3d object reconstruction from a single image. In *Proceedings of the IEEE conference on computer vision and pattern recognition*, pages 605–613, 2017. 6, 11
- [5] Chen Feng, Yuichi Taguchi, and Vineet R Kamat. Fast plane extraction in organized point clouds using agglomerative hierarchical clustering. In *2014 IEEE International Conference on Robotics and Automation (ICRA)*, pages 6218–6225. IEEE, 2014. 4
- [6] Meng-Hao Guo, Junxiong Cai, Zheng-Ning Liu, Tai-Jiang Mu, Ralph Robert Martin, and Shimin Hu. Pct: Point cloud transformer. *Comput. Vis. Media*, 7:187–199, 2021. 2, 6, 7
- [7] Abdullah Hamdi, Sara Rojas, Ali Thabet, and Bernard Ghanem. Advpc: Transferable adversarial perturbations on 3d point clouds. In *European Conference on Computer Vision*, pages 241–257. Springer, 2020. 1, 2, 6, 11
- [8] Qidong Huang, Xiaoyi Dong, Dongdong Chen, Hang Zhou, Weiming Zhang, and Nenghai Yu. Shape-invariant 3d adversarial point clouds. In *Proceedings of the IEEE/CVF Conference on Computer Vision and Pattern Recognition*, pages 15335–15344, 2022. 1, 2, 11
- [9] Jaeyeon Kim, Binh-Son Hua, Duc Thanh Nguyen, and Sai-Kit Yeung. Minimal adversarial examples for deep learning on 3d point clouds. *2021 IEEE/CVF International Conference on Computer Vision (ICCV)*, pages 7777–7786, 2021. 2
- [10] Diederik P Kingma and Jimmy Ba. Adam: A method for stochastic optimization. *arXiv preprint arXiv:1412.6980*, 2014. 11
- [11] Kaidong Li, Ziming Zhang, Cuncong Zhong, and Guanghui Wang. Robust structured declarative classifiers for 3d point clouds: Defending adversarial attacks with implicit gradients. In *Proceedings of the IEEE International Conference on Computer Vision*, 2022. 1, 3
- [12] Binbin Liu, Jinlai Zhang, and Jihong Zhu. Boosting 3d adversarial attacks with attacking on frequency. *IEEE Access*, 10:50974–50984, 2022. 1, 2, 6, 11
- [13] Daniel Liu, Ronald Yu, and Hao Su. Extending adversarial attacks and defenses to deep 3d point cloud classifiers. In *2019 IEEE International Conference on Image Processing (ICIP)*, pages 2279–2283. IEEE, 2019. 3
- [14] Zhijian Liu, Haotian Tang, Yujun Lin, and Song Han. Point-voxel cnn for efficient 3d deep learning. *Advances in Neural Information Processing Systems*, 32, 2019. 6
- [15] Shitong Luo and Wei Hu. Diffusion probabilistic models for 3d point cloud generation. In *Proceedings of the IEEE/CVF Conference on Computer Vision and Pattern Recognition*, pages 2837–2845, 2021. 3
- [16] Aleksander Madry, Aleksandar Makelov, Ludwig Schmidt, Dimitris Tsipras, and Adrian Vladu. Towards deep learning models resistant to adversarial attacks. In *6th International Conference on Learning Representations*, 2018. 2, 6, 11
- [17] Weili Nie, Brandon Guo, Yujia Huang, Chaowei Xiao, Arash Vahdat, and Anima Anandkumar. Diffusion models for adversarial purification. In *International Conference on Machine Learning (ICML)*, 2022. 3
- [18] Songyou Peng, Michael Niemeyer, Lars Mescheder, Marc Pollefeys, and Andreas Geiger. Convolutional occupancy networks. In *European Conference on Computer Vision*, pages 523–540, 2020. 11
- [19] C. Qi, Hao Su, Kaichun Mo, and Leonidas J. Guibas. Pointnet: Deep learning on point sets for 3d classification and segmentation. *2017 IEEE Conference on Computer Vision and Pattern Recognition (CVPR)*, pages 77–85, 2017. 2, 6, 7, 11
- [20] Radu Bogdan Rusu, Zoltan Csaba Marton, Nico Blodow, Mihai Dolha, and Michael Beetz. Towards 3d point cloud based object maps for household environments. *Robotics and Autonomous Systems*, 56(11):927–941, 2008. 3, 6, 11
- [21] Zhenbo Shi, Zhi Chen, Zhenbo Xu, Wei Yang, Zhidong Yu, and Liusheng Huang. Shape prior guided attack: Sparser perturbations on 3d point clouds. In *AAAI*, 2022. 2
- [22] Jascha Sohl-Dickstein, Eric Weiss, Niru Maheswaranathan, and Surya Ganguli. Deep unsupervised learning using nonequilibrium thermodynamics. In *International Conference on Machine Learning*, pages 2256–2265. PMLR, 2015. 3
- [23] Jiachen Sun, Yulong Cao, Christopher Bongsoo Choy, Zhiding Yu, Anima Anandkumar, Zhuoqing Morley Mao, and Chaowei Xiao. Adversarially robust 3d point cloud recognition using self-supervisions. In *NeurIPS*, 2021. 1, 3
- [24] Jiachen Sun, Weili Nie, Zhiding Yu, Z Morley Mao, and Chaowei Xiao. Pointdp: Diffusion-driven purification against adversarial attacks on 3d point cloud recognition. *arXiv preprint arXiv:2208.09801*, 2022. 8
- [25] Tzungyu Tsai, Kaichen Yang, Tsung-Yi Ho, and Yier Jin. Robust adversarial objects against deep learning models. In *Proceedings of the AAAI Conference on Artificial Intelligence*, volume 34, pages 954–962, 2020. 1, 2, 6, 11
- [26] Laurens Van der Maaten and Geoffrey Hinton. Visualizing data using t-sne. *Journal of machine learning research*, 9(11), 2008. 8
- [27] Jinyi Wang, Zhaoyang Lyu, Dahua Lin, Bo Dai, and Hongfei Fu. Guided diffusion model for adversarial purification. *ArXiv*, abs/2205.14969, 2022. 3
- [28] Yue Wang, Yongbin Sun, Ziwei Liu, Sanjay E. Sarma, Michael M. Bronstein, and Justin M. Solomon. Dynamic graph cnn for learning on point clouds. *ACM Transactions on Graphics (TOG)*, 38:1 – 12, 2019. 2, 6, 7
- [29] Yuxin Wen, Jiehong Lin, Ke Chen, CL Philip Chen, and Kui Jia. Geometry-aware generation of adversarial point clouds. *IEEE Transactions on Pattern Analysis and Machine Intelligence*, 2020. 1, 2
- [30] Wenxuan Wu, Zhongang Qi, and Fuxin Li. Pointconv: Deep convolutional networks on 3d point clouds. *2019 IEEE/CVF Conference on Computer Vision and Pattern Recognition (CVPR)*, pages 9613–9622, 2019. 2, 6, 7
- [31] Ziyi Wu, Yueqi Duan, He Wang, Qingnan Fan, and Leonidas J Guibas. If-defense: 3d adversarial point cloud defense via implicit function based restoration. *arXiv preprint arXiv:2010.05272*, 2020. 1, 2, 3, 6, 11

- [32] Zhirong Wu, Shuran Song, Aditya Khosla, Fisher Yu, Linguang Zhang, Xiaoou Tang, and Jianxiong Xiao. 3d shapenets: A deep representation for volumetric shapes. In *Proceedings of the IEEE conference on computer vision and pattern recognition*, pages 1912–1920, 2015. 6, 11
- [33] Chong Xiang, Charles R Qi, and Bo Li. Generating 3d adversarial point clouds. In *Proceedings of the IEEE Conference on Computer Vision and Pattern Recognition*, pages 9136–9144, 2019. 1, 2, 6, 11
- [34] Tiange Xiang, Chaoyi Zhang, Yang Song, Jianhui Yu, and Weidong Cai. Walk in the cloud: Learning curves for point clouds shape analysis. *2021 IEEE/CVF International Conference on Computer Vision (ICCV)*, pages 895–904, 2021. 2, 6, 7
- [35] Jiancheng Yang, Qiang Zhang, Rongyao Fang, Bingbing Ni, Jinxian Liu, and Qi Tian. Adversarial attack and defense on point sets. *arXiv preprint arXiv:1902.10899*, 2019. 3, 5, 6, 11
- [36] Li Yi, Vladimir G Kim, Duygu Ceylan, I-Chao Shen, Mengyan Yan, Hao Su, Cewu Lu, Qixing Huang, Alla Sheffer, and Leonidas Guibas. A scalable active framework for region annotation in 3d shape collections. *ACM Transactions on Graphics (ToG)*, 35(6):1–12, 2016. 6, 11
- [37] Tianhang Zheng, Changyou Chen, Junsong Yuan, Bo Li, and Kui Ren. Pointcloud saliency maps. In *Proceedings of the IEEE/CVF International Conference on Computer Vision*, pages 1598–1606, 2019. 2, 6, 11
- [38] Hang Zhou, Dongdong Chen, Jing Liao, Kejiang Chen, Xiaoyi Dong, Kunlin Liu, Weiming Zhang, Gang Hua, and Nenghai Yu. Lg-gan: Label guided adversarial network for flexible targeted attack of point cloud based deep networks. In *Proceedings of the IEEE/CVF Conference on Computer Vision and Pattern Recognition*, pages 10356–10365, 2020. 2
- [39] Hang Zhou, Kejiang Chen, Weiming Zhang, Han Fang, Wenbo Zhou, and Nenghai Yu. Dup-net: Denoiser and up-sampler network for 3d adversarial point clouds defense. In *Proceedings of the IEEE International Conference on Computer Vision*, pages 1961–1970, 2019. 1, 3, 6, 11
- [40] Linqi Zhou, Yilun Du, and Jiajun Wu. 3d shape generation and completion through point-voxel diffusion. In *Proceedings of the IEEE/CVF International Conference on Computer Vision*, pages 5826–5835, 2021. 3, 6

Appendix A. Details of Experiment Setup

Datasets. We conducted experiments on two main datasets, namely, ModelNet40 [32] and ShapeNet Part [36], respectively. ModelNet40 [32] is the most commonly-used dataset for evaluating point cloud recognition and contains 12,311 CAD models belonging to 40 semantic categories, of which 2,468 are used for testing. ShapeNet Part [36] has 16 categories, including a total of 16,846 objects, of which 2,874 were used for testing. To generate adversarial point clouds in a uniform standard, for both datasets, we sample 1,024 points uniformly from the surface of each original point cloud following [19] and [8], and normalize them to a unit ball.

Attacks. We have selected five attack methods for generating adversarial point clouds with different degrees of distortion. For 3D-Adv [33], we use the L_2 distance as a perturbation constraint and perform 10 binary searches with 200 iterations for each search. The weight of the L_2 loss is initially 10 and maximum 80. k NN-Adv [25] uses the Chamfer measurement [4] between the adversarial point cloud and the clean point cloud and k -nearest neighbors loss to constrain the perturbations with weights of 5 and 3, respectively. We use the Adam [10] optimizer to optimize 1000 times with an initial learning rate of 0.001. The PGD [16] attack is one of the strongest attacks on neural networks and is also applicable to 3D point clouds. We follow the setup of [8] with 50 iterations and the step size is set to 0.007 to attack the 3D point cloud recognition model. AdvPC [7] uses an additional auto-encoder before the classifier to mitigate the overfitting of the adversarial point cloud to the model, where we adopt $\gamma=0.25$ and iterate 1000 times. AOF [12] combines the low-frequency component in the adversarial loss used to generate the adversarial point cloud to improve the transferability. We follow the default settings in the paper. We use BPDA [2] to perform white-box attacks. Specifically, during the backward propagation of computing the gradient, we obey the assumption that $\mathcal{D}(\mathbf{x}) \approx \mathbf{x}$ where \mathcal{D} represents the proposed defense method. The gradient is still an approximate value even after many iterations, so it is not the optimal adaptive attack and can still be improved in future work. For the above attacks, we restrict the maximum value of the perturbation distance to 0.18. We set 200 points to be discarded for the point dropping [37] attack, namely, Drop-200.

Defenses. Given a point cloud with N points, we randomly sample $(N - 500)$ points for SRS [35] defense. SOR [20] is the statistical filtering method to remove outliers, and we follow the default settings in [39]. We set the upsampling ratio to 4 for DUP-Net [39], i.e. 4096 points for the final output. IF-Defense [31] utilizes the prior of

implicit functions and has the best defensive performance among present pre-processing methods. We optimize 200 times of this defense based on ConvONet [18], following the settings of its paper.

Appendix B. More Results

Quantitative Results. In Tables 6 to 9, we provide more comparison results of different models on ModelNet40 under different attacks. The proposed approach outperforms present defenses against large distortion attacks while maintaining comparable performance in the face of slight distortions.

Distortion Estimation for Different Attacks. In Figure 6, we provide the number of samples for different attack methods at each diffusion time step after distortion estimation. It can be observed from the figure that for attacks with large distortion such as AdvPC, the vast majority of samples use the maximum budgeted diffusion time step while for attacks with less distortion such as 3D-Adv, only a small number of samples use a large diffusion time step, which can improve the robust classification accuracy for shape invariant adversarial point clouds. Although effective, the robust classification accuracy in the small distortion case can be further improved in the future, since the distortion estimates of clean point clouds are also large in some cases and artificially divided intervals are used.

| | Clean | 3D-Adv | k NN-Adv | PGD | AdvPC | AOF | Drop-200 |
|------------|-------------|-------------|-------------|-------------|-------------|-------------|-------------|
| No defense | 89.0 | 0 | 6.44 | 0 | 0 | 0 | 38.9 |
| SRS | 89.3 | 87.6 | 82.6 | 72.0 | 7.78 | 1.7 | 42.1 |
| SOR | 89.4 | 88.2 | 80.1 | 78.8 | 47.5 | 5.39 | 42.7 |
| DUP-Net | 88.1 | 87.8 | 84.1 | 83.1 | 63.3 | 14.3 | 46.1 |
| IF-Defense | 87.4 | 87.3 | 86.5 | 86.9 | 81.5 | 54.8 | 55.5 |
| Ada3Diff | 89.0 | 86.9 | 86.2 | 85.9 | 85.0 | 84.1 | 55.1 |

Table 6. Comparison of robust classification accuracy of PointNet on ModelNet40 under different attacks.

| | Clean | 3D-Adv | k NN-Adv | PGD | AdvPC | AOF | Drop-200 |
|------------|-------------|-------------|-------------|-------------|-------------|-------------|-------------|
| No defense | 92.3 | 0 | 2.80 | 0 | 2.1 | 0 | 69.1 |
| SRS | 83.5 | 80.5 | 78 | 69.3 | 24.7 | 17.4 | 46.1 |
| SOR | 91.3 | 87.4 | 72.7 | 70.3 | 23.6 | 12.7 | 70.9 |
| DUP-Net | 64.0 | 59.4 | 46.8 | 44.6 | 20.1 | 13.3 | 43.5 |
| IF-Defense | 84.2 | 84.4 | 84.0 | 83.1 | 70.3 | 51.7 | 72.7 |
| Ada3Diff | 87.2 | 86.7 | 86.4 | 85.9 | 85.9 | 85.3 | 75.6 |

Table 7. Comparison of robust classification accuracy of DGCNN on ModelNet40 under different attacks.

| | Clean | 3D-Adv | k NN-Adv | PGD | AdvPC | AOF | Drop-200 |
|------------|-------------|-------------|-------------|-------------|-------------|-------------|-------------|
| No defense | 92.7 | 75.6 | 7.74 | 0.28 | 0.53 | 2.15 | 66.9 |
| SRS | 91.8 | 90.9 | 79.9 | 74.0 | 32.9 | 20.3 | 69.4 |
| SOR | 91.8 | 91.7 | 66.9 | 62.2 | 29.2 | 12.8 | 71.3 |
| DUP-Net | 85.0 | 82.9 | 72.9 | 63.0 | 31.8 | 21.9 | 59 |
| IF-Defense | 88.9 | 88.9 | 86.1 | 82.7 | 67.8 | 57.1 | 71.4 |
| Ada3Diff | 87.4 | 87.6 | 86.9 | 86.5 | 85.5 | 85.8 | 71.8 |

Table 8. Comparison of robust classification accuracy of PCT on ModelNet40 under different attacks.

| | Clean | 3D-Adv | k NN-Adv | PGD | AdvPC | AOF | Drop-200 |
|------------|-------------|-------------|-------------|-------------|-------------|-------------|-------------|
| No defense | 91.9 | 0 | 7.62 | 0 | 0.41 | 0 | 78 |
| SRS | 90.7 | 88.7 | 79.5 | 71.1 | 12.1 | 11.6 | 71.2 |
| SOR | 91.3 | 90.4 | 71.8 | 49.8 | 3.9 | 5.31 | 78.7 |
| DUP-Net | 84.1 | 82.2 | 78.2 | 69.2 | 32.9 | 33.3 | 68.6 |
| IF-Defense | 89.7 | 89.2 | 88.0 | 85.0 | 46.6 | 43.6 | 76.9 |
| Ada3Diff | 86.8 | 86.9 | 86.5 | 86.3 | 83.4 | 83.5 | 69.7 |

Table 9. Comparison of robust classification accuracy of PointConv on ModelNet40 under different attacks.

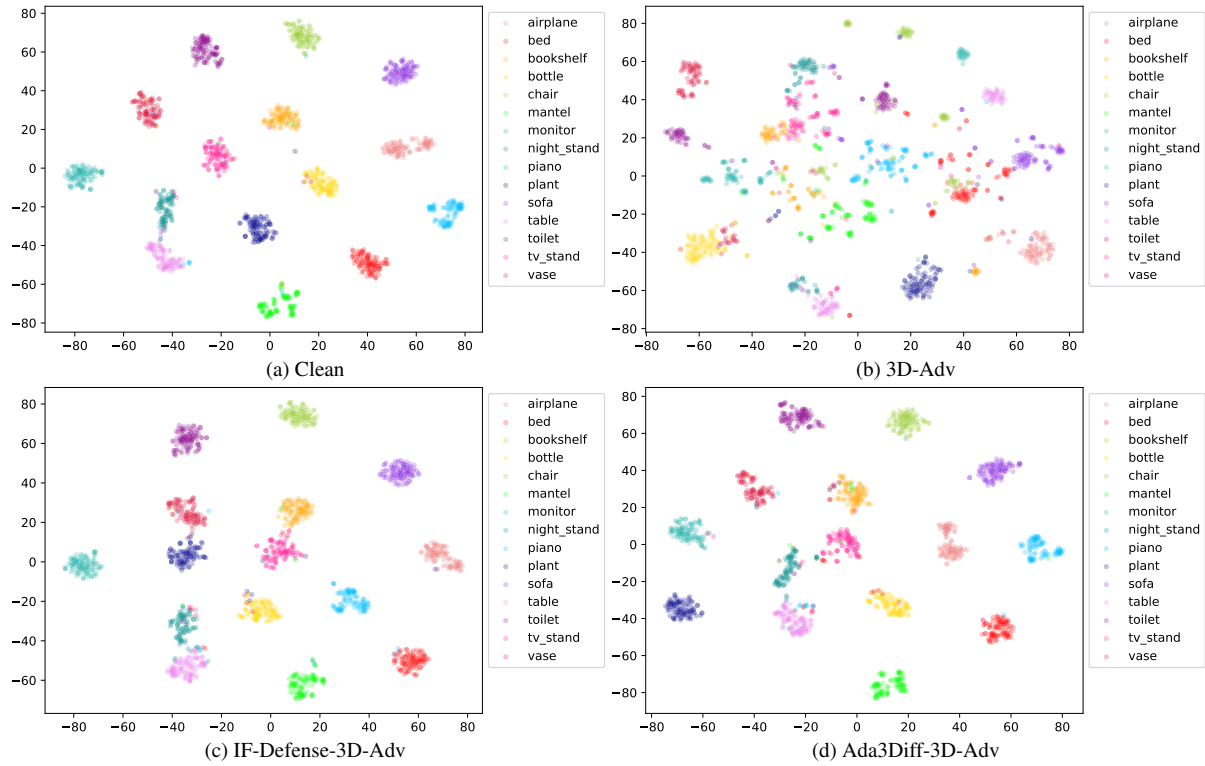


Figure 5. The t-SNE visualizations of the latent space. (a) and (b) are the feature distributions visualized for the clean point cloud and the 3D-Adv adversarial point cloud, respectively. (c) and (d) are the latent distributions of the adversarial point clouds after IF-Defense and Ada3Diff defense, respectively.

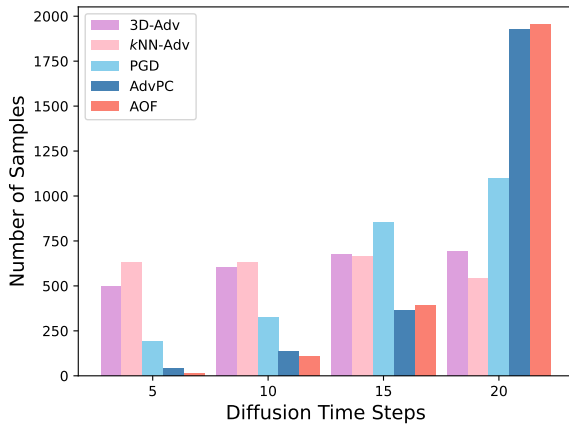


Figure 6. Statistical information on the distortion estimates of different attacks.

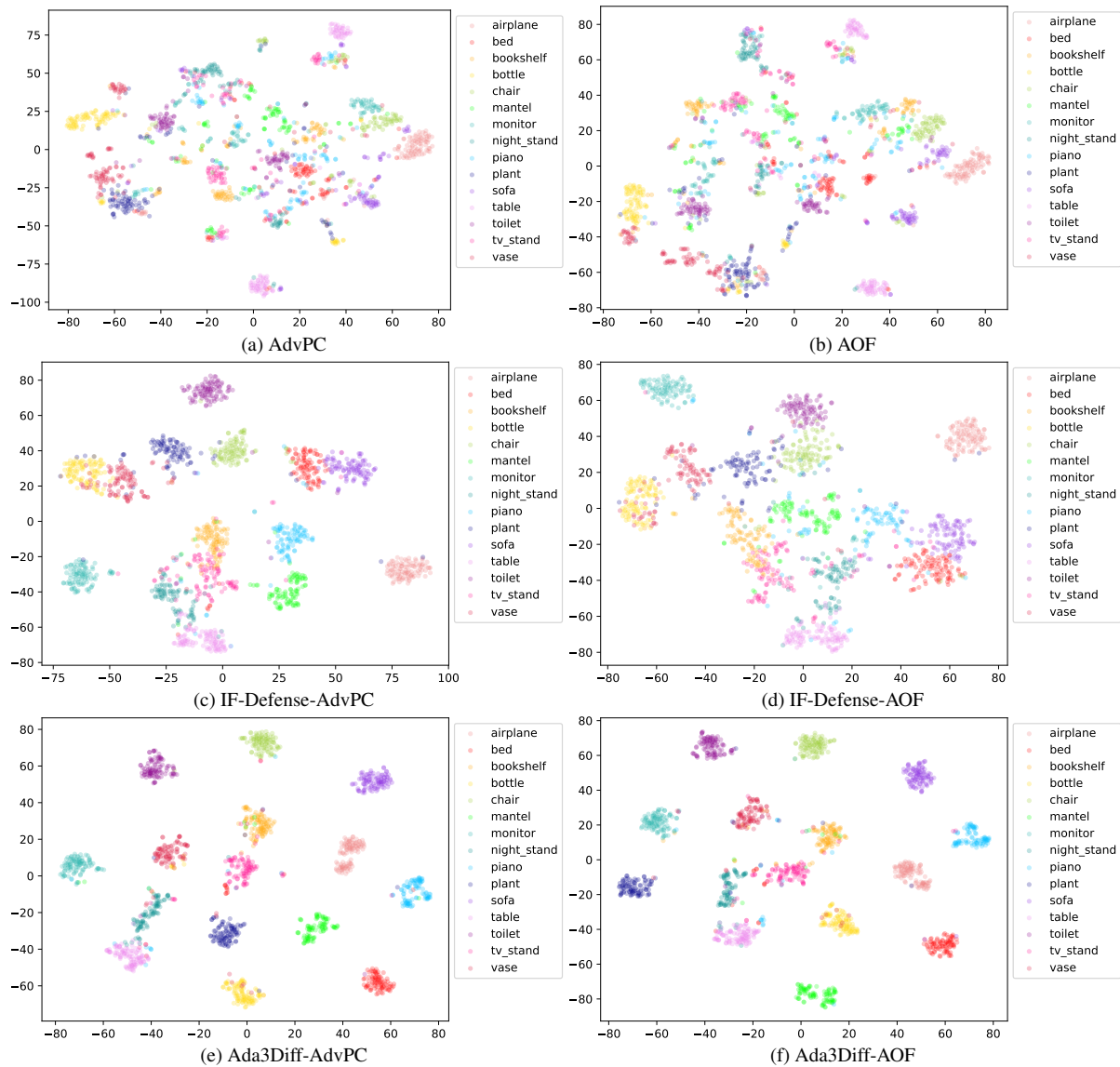


Figure 7. The t-SNE visualizations of the latent space. The first row shows the visualization results of the adversarial point cloud, and the second and third rows show the latent distributions of the point cloud reconstructed by other defense methods and our method, respectively.